

Synchronization is Enhanced in Weighted Complex Networks

M. Chavez,^{1,2} D.-U. Hwang,¹ A. Amann,^{1,3} H. G. E. Hentschel,⁴ and S. Boccaletti¹

¹*Istituto Nazionale di Ottica Applicata, Largo E. Fermi, 6 - 50125 Florence, Italy*

²*Laboratoire de Neurosciences Cognitives et Imagerie Cérébrale (LENA) CNRS UPR-640, Hôpital de la Salpêtrière, 47 Bd. de l'Hôpital, 75651 Paris CEDEX 13, France*

³*Institut für Theoretische Physik, Technische Universität Berlin, Hardenbergstr. 36, 10623 Berlin, Germany*

⁴*Physics Department, Emory University, Atlanta, Georgia 30322, USA*

(Received 22 November 2004; published 2 June 2005)

The propensity for synchronization of complex networks with directed and weighted links is considered. We show that a weighting procedure based upon the global structure of network pathways enhances complete synchronization of identical dynamical units in scale-free networks. Furthermore, we numerically show that very similar conditions hold also for phase synchronization of nonidentical chaotic oscillators.

DOI: 10.1103/PhysRevLett.94.218701

PACS numbers: 89.75.Hc, 89.75.-k, 05.45.Xt, 87.18.Sn

Networks of dynamical units constitute models of many natural systems. Examples range from biological and chemical oscillators to electrical power grids and transportation networks [1]. Many of these networks exhibit complex topological properties such as the small-world and scale-free properties [2]. Small-world (SW) networks [3] are objects in between regular and random networks characterized by a small average distance between any two nodes (scaling logarithmically rather than linearly with the network size), while keeping a relatively highly clustered structure. Scale-free (SF) networks [4] are examples of SW networks displaying a power-law distribution $p(k) \sim k^{-\gamma}$ in the node connectivity k (degree).

In recent years, complex networks have provided a fresh and increasingly challenging framework for the study of collective (synchronized) behaviors, based on the interplay between complexity in the overall topology and local dynamical properties of the coupled units. As an example, SW wirings have been proven to enhance synchronization as compared with regular topologies [5,6]. Initially, this enhancement was attributed to the decreasing of the smaller average network distance between nodes. In fact, synchronization can be affected by several other quantities, as recently manifested in Ref. [7], where increasing the heterogeneity in the connectivity distribution at the same average network distance eventually leads to a deterioration of synchrony [7].

A basic assumption of previous works is that the local units are symmetrically coupled with undirected coupling strengths (unweighted links). However, in many circumstances this simplification does not match the peculiarities of real networks. In ecological systems, for instance, the nonuniform weight in prey-predator interactions plays a crucial role in the food web dynamics [8]. The traffic load of a road, or the number of passengers in subways lines or airports, are critical quantities in the study of transportation networks [9]. Similarly, the natural differences of neurons and their dendritic connections result in distinct capabilities

of transmission and information processing in neural networks [10].

In this Letter, we give evidence of the constructive role of asymmetric and weighted wirings on the synchronization of coupled oscillators. By exploiting the global structure of shortest paths among nodes in the wiring, the weight of a link will be related to its load, which measures the fraction of shortest paths in the network that are making use of that connection, and is qualitatively related to the traffic of communication passing through it [11]. Namely, (i) we assess the network propensity for synchronization (PFS) via the distribution of the coupling matrix eigenvalue spectra [6,12] as a function of the relative importance of the link loads, and (ii) we give evidence that varying the weighting procedure gives optimal conditions for synchronization in a class of SF networks with different degree distributions. Moreover, we find a suitable generalization of this procedure to optimize the phase synchronization of nonidentical oscillators.

We start by considering a network of N linearly coupled identical oscillators. The equation of motion reads

$$\dot{\mathbf{x}}_i = \mathbf{F}(\mathbf{x}_i) - \sigma \sum_{j=1}^N G_{ij} \mathbf{H}[\mathbf{x}_j], \quad i = 1, \dots, N, \quad (1)$$

where $\dot{\mathbf{x}} = \mathbf{F}(\mathbf{x})$ governs the local dynamics of the vector field \mathbf{x}_i in each node, $\mathbf{H}[\mathbf{x}]$ is a linear vectorial function, σ is the coupling strength, and G is a coupling matrix.

Let us consider the case where G has a real spectrum (as, e.g., in symmetric coupling). Stability of the synchronous state $[\mathbf{x}_i(t) = \mathbf{x}_s(t), \forall i]$ can be accounted for by diagonalizing the linear stability equation, yielding N blocks of the form $\dot{\zeta}_i = \mathbf{J}\mathbf{F}(\mathbf{x}_s)\zeta_i - \sigma\lambda_i\mathbf{H}[\zeta_i]$ (where \mathbf{J} is the Jacobian operator). The blocks only differ by $\lambda_1 \leq \dots \leq \lambda_i \leq \dots \leq \lambda_N$ (the eigenvalues of G). Replacing $\sigma\lambda_i$ by ν in the equation, the behavior of the largest Lyapunov exponent vs ν [also called master stability function [12] (MSF)] fully accounts for linear stability of the synchronization manifold. Namely, the synchronized state (asso-

ciated with λ_1), is stable if all the remaining blocks (associated with λ_i , $i = 2, \dots, N$) have negative Lyapunov exponents. For a large class of oscillatory systems, the MSF is negative in a finite parameter interval $I_{\text{st}} \equiv (\nu_1 \leq \nu \leq \nu_2)$ [12]. The stability condition is satisfied when the whole set of eigenvalues (multiplied by σ) enters the interval I_{st} . This is accomplished when *simultaneously* $\sigma\lambda_2 > \nu_1$ and $\sigma\lambda_N < \nu_2$. As ν_2 and ν_1 depend on the specific choice of $\mathbf{F}(\mathbf{x})$ and $\mathbf{H}[\mathbf{x}]$, the key quantity for assessing PFS of a network is the eigenratio λ_N/λ_2 , which only depends on the topology of the network. The smaller λ_N/λ_2 is, the more packed the eigenvalues of G are, leading to an enhanced σ interval for which stability is obtained for any choice of $\mathbf{F}(\mathbf{x})$ and $\mathbf{H}[\mathbf{x}]$ [6].

A first attempt at assessing enhancement of synchronization due to weighted connections was proposed in Ref. [13], where the coupling factor in the right hand side of Eq. (1) was taken to be $\frac{\sigma}{k_i^B} \sum_{j=1}^N M_{ij} \mathbf{H}[\mathbf{x}_j]$ (M_{ij} being the Laplacian matrix). This asymmetric wiring provides a spectrum of real eigenvalues, and an optimal condition $\beta = 1$ for synchronization was found [13]; note that such a weighting procedure only retains information on the local features of the network (the node degree).

We show that further enhancement in synchronization can be achieved by exploiting the information contained in the overall topology, i.e., by scaling the coupling strength to the load of each link. The load ℓ_{ij} of the link connecting nodes i and j quantifies the traffic of shortest paths that are making use of that link [11], and therefore it reflects the network structure at a global scale (its value can be strongly influenced by pairs of nodes that may be very far away from either nodes i and j). Precisely, for each pair of nodes i', j' in the network, we count the number $n(i', j')$ of shortest paths connecting them. For each one of such shortest paths, we then add $1/n$ to the load of each link forming it. A schematic example of such weighting procedure is sketched in Fig. 1.

The network equation reads:

$$\dot{\mathbf{x}}_i = \mathbf{F}(\mathbf{x}_i) - \frac{\sigma}{\sum_{j \in K_i} \ell_{ij}^\alpha} \sum_{j \in K_i} \ell_{ij}^\alpha \mathbf{H}[\mathbf{x}_j], \quad (2)$$

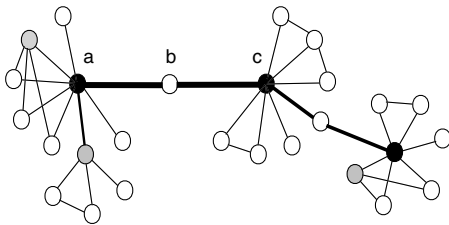


FIG. 1. Schematic representation of the weighting procedure. The link thickness is proportional to the link load, while the node colors reflect the node degrees (white, black, and gray correspond to nodes with low, high, and medium degrees, respectively). In general, nodes with low degrees (like node b) may have links with very high loads, and nodes with high degrees (like nodes a and c) may have links with low loads.

where α is a real tunable parameter, and K_i is the set of neighbors to the i th node.

An important property of our coupling scheme is the nature of the coupling matrix G , defined by comparing Eq. (2) with Eq. (1). The diagonal elements of G are always normalized to one. Such normalization prevents the coupling term from being arbitrarily large (or arbitrarily small) for all possible network topologies, thus making it a meaningful realization of what happens in many real world situations (as, e.g., neuronal networks) where the local influence of the environment on the dynamics does not scale with the number of connections. Although G is asymmetric for all α , it can be written as a product $G = QL$, where L is a zero row-sum matrix with off-diagonal entries $L_{ij} = -\ell_{ij}^\alpha$, and $Q = \text{diag}\{\frac{1}{\sum_j \ell_{ij}^\alpha}, \dots, \frac{1}{\sum_j \ell_{Nj}^\alpha}\}$. Using matrix identities [14], the eigenvalue spectrum of G is the same as that obtained from the matrix $W = Q^{1/2} L Q^{1/2}$, and therefore is real with nonnegative values, and all the arguments of the MSF approach apply. Moreover, because G has a zero row sum, the smallest eigenvalue λ_1 is zero [14], while $\lambda_2 > 0$ for connected networks, and $\lambda_i \leq 2\forall i$ [14,15]. Furthermore, Gerschgorin's circle theorem [16] guarantees in our case that the relationship $0 < \lambda_2 \leq \lambda_N \leq 2$ holds for connected networks independently on the network size N . Another important point to be stressed concerns the various limits the coupling term can assume when changing α . The limit $\alpha = 0$ corresponds to the best synchronizability condition of Ref. [13]. From Eq. (2) we see that in the limit $\alpha = +\infty$ ($\alpha = -\infty$) only the links with the largest (smallest) loads ℓ_{ij} are selected as the incoming links for each node i . Therefore this induces a network with at least N directed links, which can be either connected or disconnected. In the connected (disconnected) case, the ratio λ_N/λ_2 will be equal to 2 ($+\infty$), thus yielding a very strong (very weak) condition for synchronization.

By varying α in Eq. (2), and by monitoring the ratio λ_N/λ_2 of the coupling matrix G , we can now study the PFS of a class of SF networks with different degree distributions, as well as of random networks. The used class of scale-free networks is obtained by a generalization of the preferential attachment growing procedure introduced in Ref. [4]. Namely, starting from $m + 1$ all to all connected nodes, at each time step a new node is added with m links. These m links point to old nodes with probability $p_i = \frac{k_i + B}{\sum_j (k_j + B)}$, where k_i is the degree of the node i , and B is a tunable real parameter, representing the initial attractiveness of each node. This procedure allows a selection of the γ exponent of the power-law scaling in the degree distribution [2] [$p(k) \sim k^{-\gamma(B,m)}$], with $\gamma(B,m) = 3 + \frac{B}{m}$ in the thermodynamic ($N \rightarrow \infty$) limit. While the average degree is by construction $\langle k \rangle = 2m$ (thus independent on B), the heterogeneity of the degree distribution can be strongly modified by B . This induces convergence of higher order moments of $p(k)$, in contrast with the case $B = 0$, that recovers the preferential attachment rule originally introduced in Ref. [4].

Figure 2(a) shows the logarithm of λ_N/λ_2 in the parameter space (α, B) for SF networks. The first crucial observation is that the surface of λ_N/λ_2 has a pronounced minimum at $0 < \tilde{\alpha} \approx 1$ for all values of B above a given $B_c > 0$. Because here $\alpha = 0$ recovers the optimal condition when only the information on node degrees is used (the condition $\beta = 1$ in Ref. [13]), this indicates that our weighting procedure based on the link loads *always* enhances the network PFS. This is quantified in Fig. 2(b), where we report the quantity $\Gamma = \log(\lambda_N/\lambda_2) - [\log(\lambda_N/\lambda_2)]_{\alpha=0}$ in the parameter space. The large region of negative values of Γ corresponds to topological structures (B) and weighting configurations (α) providing better synchronization propensities than a weighting process based on the node degrees.

This result indicates that conveying the global complex structure of shortest paths into a weighting procedure gives in that range a better criterion for synchronization than solely relying on the local information around a node. With increasing α , the enhancement region is limited for $B > B_c$ [see the upper black line in Fig. 2(b)]. The reason for this is that increasing α above $\tilde{\alpha}$ introduces two effects: the first is that it makes it more likely that a unidirected tree structure appears in the network, and the second is that it increases the chance of disconnecting the network. These two effects are competing to determine synchronous behavior, insofar as the former increases the likelihood of synchronization only if the network remains connected. Therefore, a second critical value $\alpha_c(B) > \tilde{\alpha}$ can be expected such that the disconnection mechanism dominates the tree structure induction if $B > B_c$. In all our results, N

has been varied from 500 to 1000 without significant qualitative differences.

While our study focused on $m = 2$, results for larger m values (not reported here) show the following changes in the scenario: increasing m diminishes the value of $\tilde{\alpha}$, and it increases the likelihood of disconnecting the network in the limit $\alpha \rightarrow \infty$, thus inducing $B_c \rightarrow 0$. In the opposite limit, $m = 1$ always ensures that the network remains connected at $\alpha \rightarrow \infty$, regardless of B .

For comparison, we also apply our coupling scheme to a class of networks with high homogeneous degree distribution, represented by random networks obtained as in Ref. [3]. Precisely, starting from a ring lattice of N nodes connected with their $m = 2$ nearest neighbors, each nearest neighbor connection is substituted with probability $0 \leq p \leq 1$ by a link that points randomly to another node in the network. The situation with random networks ($p = 1$) is illustrated in Fig. 3. Figure 3(a) reports the behavior of $\log(\lambda_N/\lambda_2)$ vs α , indicating that here also our weighting procedure based on link loads enhances the network PFS (the minimum of the curve is always positioned at $0 < \tilde{\alpha} \approx 1$); while Fig. 3(b) reports the comparative quantity $\Gamma_c = [\log(\lambda_N/\lambda_2)]_{\text{SF}} - [\log(\lambda_N/\lambda_2)]_{\text{random}}$ in the parameter space (α, B) , indicating that for all $\alpha > 0$ weighted SF configurations provide better topologies for inducing a synchronized behavior than random networks. The analysis of the whole SW regime ($0 < p < 1$) reveals that PFS in general increases with p , but still the minimum of λ_N/λ_2 remains at $\tilde{\alpha} \approx 1$. A more detailed account of this regime will be reported elsewhere.

It is crucial to emphasize that the conditions for optimal synchronization discussed so far rigorously apply only for

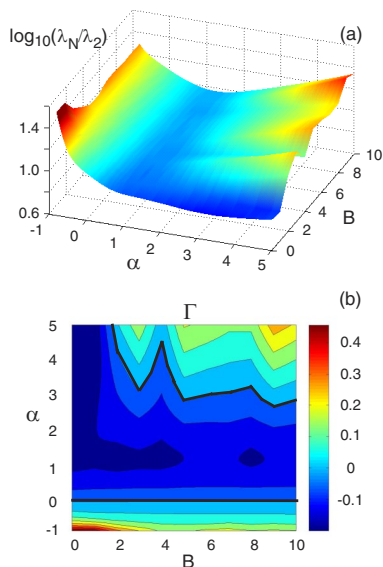


FIG. 2 (color online). (a) λ_N/λ_2 (in logarithmic scale) for SF networks vs the dimensionless parameter space (α, B) . (b) Γ (see text for definition) vs (α, B) . In all cases $m = 2$, and the graphs refer to averaging over 10 realizations of networks with $N = 1000$. The domain with $\Gamma < 0$ is outlined by the black contours drawn on the figure.

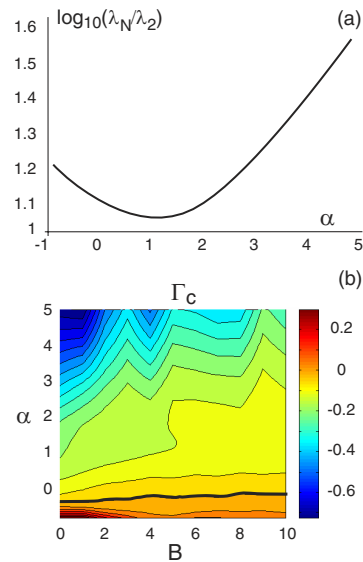


FIG. 3 (color online). (a) λ_N/λ_2 (in logarithmic scale) for random graphs vs α . (b) Γ_c (see text for definition) vs (α, B) . Random networks have $\langle k \rangle = 2m = 4$, identical to that of SF networks. In the domain where $\Gamma_c < 0$ SF networks synchronize better than random networks. Same stipulations as in the caption of Fig. 2.

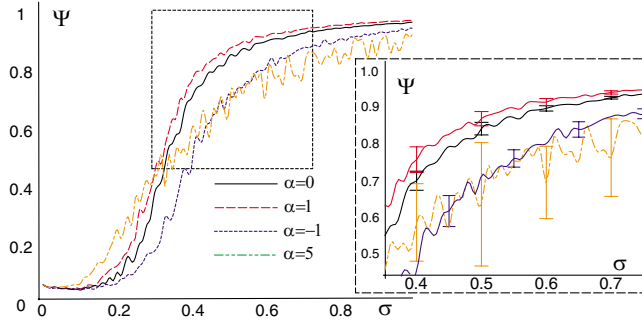


FIG. 4 (color online). The phase order parameter Ψ (see text for definition) vs σ for nonidentical chaotic Rössler oscillators. All parameters are specified in the text. Data refer to averages over 10 different realizations of SF networks with $B = 10$, $m = 2$, and $N = 1000$. The inset is a zoom of the dashed region, with the corresponding error bars.

complete synchronization [17] of identical systems [6,12]. Considering a complex network of coupled nonidentical oscillators is, however, very relevant for many practical situations. In this case, the theory of MSF cannot be applied, since (i) for nonidentical systems a complete synchronization invariant manifold ($\mathbf{x}_i = \mathbf{x}_s, \forall i$) cannot be defined and (ii) such systems may also display weaker degrees of synchronization, such as phase synchronization [17]. Nevertheless, numerical evidence shows that the eigenratio λ_N/λ_2 still provides a qualitative description in this case. Indeed, we implemented a SF network of nonidentical chaotic Rössler oscillators. The dynamics is ruled by Eq. (2), with $\mathbf{x}_i = (x_i, y_i, z_i)$, $\mathbf{F}(\mathbf{x}_i) = \mathbf{F}_i(\mathbf{x}_i) = [-\omega_i y_i - z_i, \omega_i x_i + 0.165 y_i, 0.2 + z_i(x_i - 10)]$, and $\mathbf{H}[\mathbf{x}] = x$. Here ω_i is the natural frequency of the i th oscillator, which is randomly assigned from a Gaussian distribution with mean value $\omega_{\text{mean}} = 1$ and standard deviation $\Delta\omega = 0.02$.

Phase synchronization in this network can be characterized by monitoring the order parameter [17] $\Psi = \langle \frac{1}{N} |\sum_{i=1}^N e^{j\phi_i(t)}| \rangle_t$, where $\phi_i(t) = \arctan[\frac{y_i(t)}{x_i(t)}]$ denotes the instantaneous phase of the i th oscillator, and $\langle \dots \rangle_t$ stays for a time average. If all oscillators rotate independently, $\Psi \sim 1/\sqrt{N}$. In contrast, if their motions are phase synchronized then $\Psi \sim 1$.

Figure 4 shows the behavior of Ψ vs σ for $B = 10$ and for various values of α (similar results hold for other $B > 0$). Remarkably, the observed phase synchronization scenario reflects qualitatively the results of Fig. 2(b). Indeed, for $\alpha = 1$ (dashed line in Fig. 4), the σ range for which $\Psi \sim 1$ is larger and therefore provides a better phase synchronization than the case $\alpha = 0$ (continuous line). In the other two curves in Fig. 4 ($\alpha = -1$ and $\alpha = 5$) the synchronization scenario is worse than the case $\alpha = 0$. Since these α values are outside the enhancement region in Fig. 2(b), this confirms that the MSF arguments also

constitute a good criterion to assess network PFS in the case of nonidentical dynamical units. PFS is improved if the interval σ for which $\Psi \sim 1$ increases. Note that, upon variation of σ , a smooth transition towards a phase synchronized state occurs, while for identical oscillators a sharp (first order) transition is expected [18].

In conclusion, we have shown that a weighting procedure based upon the global structure of network pathways yields a PFS higher than one based on the local information of nodes. Similar conditions were numerically found for phase synchronization in networks of coupled nonidentical units. The method can therefore have applications for the modeling of real networks where the synchronization of nonidentical units occurs. Examples are the synchronized oscillations in transcriptional regulation or neural networks, the study of information flows in signaling networks, as well as epidemiological models.

Work partly supported by MIUR-FIRB Project No. RBNE01CW3M-001, and the Postdoctoral Program of Korea Science & Eng. Foundation (KOSEF).

-
- [1] S. H. Strogatz, *Nature (London)* **410**, 268 (2001); I. Z. Kiss, Y. Zhai, and J. L. Hudson, *Science* **296**, 1676 (2002).
 - [2] R. Albert and A. L. Barabási, *Rev. Mod. Phys.* **74**, 47 (2002); S. N. Doroogovtsev and J. F. F. Mendes, *Adv. Phys.* **51**, 1079 (2002).
 - [3] D. J. Watts and S. H. Strogatz, *Nature (London)* **393**, 440 (1998).
 - [4] A. L. Barabási and R. Albert, *Science* **286**, 509 (1999).
 - [5] L. F. Lago-Fernández *et al.*, *Phys. Rev. Lett.* **84**, 2758 (2000).
 - [6] B. Barahona and L. M. Pecora, *Phys. Rev. Lett.* **89**, 054101 (2002).
 - [7] T. Nishikawa *et al.*, *Phys. Rev. Lett.* **91**, 014101 (2003).
 - [8] G. A. Polis, *Nature (London)* **395**, 744 (1998).
 - [9] V. Latora and M. Marchiori, *Phys. Rev. Lett.* **87**, 198701 (2001).
 - [10] G. Buzsáki *et al.*, *Trends Neurosci.* **27**, 186 (2004).
 - [11] K. I. Goh, B. Kahng, and D. Kim, *Phys. Rev. Lett.* **87**, 278701 (2001).
 - [12] L. M. Pecora and T. L. Carroll, *Phys. Rev. Lett.* **80**, 2109 (1998).
 - [13] A. E. Motter, C. Zhou, and J. Kurths, *Europhys. Lett.* **69**, 334 (2005).
 - [14] D. M. Cvetkovic, M. Doob, and H. Sachs, *Spectra of Graphs: Theory and Applications* (Johann Ambrosius Barth Verlag, Heidelberg, 1995).
 - [15] F. Chung, L. Lu, and V. Vu, *Proc. Natl. Acad. Sci. U.S.A.* **100**, 6313 (2003).
 - [16] S. A. Gershgorin, *Bull. Acad. Sci. USSR, Leningrad* **2**, 749 (1931).
 - [17] S. Boccaletti *et al.*, *Phys. Rep.* **366**, 1 (2002).
 - [18] P. G. Lind, J. A. C. Gallas, and H. J. Herrmann, *Phys. Rev. E* **70**, 056207 (2004).